INTERCARRIER INTERFERENCE IN DSL NETWORKS DUE TO ASYNCHRONOUS DMT TRANSMISSION

Rodrigo B. Moraes, Paschalis Tsiaflakis and Marc Moonen

Dept. of Electrical Engineering (ESAT-SCD) and iMINDS Future Health Department
KU Leuven, Leuven, Belgium
E-mails: {rodrigo.moraes, paschalis.tsiaflakis , marc.moonen}@esat.kuleuven.be

ABSTRACT

We focus on the effects of intercarrier interference (ICI) in digital subscriber line (DSL) systems due to asynchronous discrete multitone (DMT) transmission and its impact on dynamic spectrum management (DSM). ICI arises when the DMT blocks of interfering users in the network are not aligned in time and it may significantly impact the system performance. Our contribution is the derivation of a simple and accurate model for the effect of the ICI. We propose both an ICI model based on the particular delay between two users and an ICI model averaged over the delays between two users. Simulation results show that an accurate characterization of the ICI positively impacts the performance of DSM solutions.

***Index Terms*—** Digital subscriber lines, dynamic spectrum management, inter-carrier interference.

1. INTRODUCTION

Digital Subscriber Line (DSL) technology is today one of the main technologies for broadband access. There has been a strong activity in the research community to deal with DSL's main problems. One such area of research is focused on the optimal allocation of per-user transmit power so that the impact of multi-user crosstalk, the main source of performance degradation for DSL, is minimized and the capabilities of the network are maximized. This is referred to as dynamic spectrum management (DSM).

Most of this previous work considers a synchronous discrete multitone (DMT) model, one in which all users have their DMT blocks perfectly synchronized. This leads to crosstalk that is decoupled across tones. This assumption simplifies the DSM optimization problem significantly. However, the synchronous DMT model may not be very realistic in practice. There are some proposals to overcome the asynchronicity of the DMT blocks by adding a cyclic suffix [1], but it must be said that the conditions for synchronous DMT transmission may not always be easy to attain. Situations where interfering users belong to different service providers or where transmitters are not co-located are especially troublesome. In this paper we therefore focus on the asynchronous DSM problem [2, 3, 4, 5].

This research work was carried out at the ESAT Laboratory of the KU Leuven, in the frame of the KU Leuven Research Council PFV/10/002 (OPTEC); Concerted Research Action GOA-MaNet; IUAP P7/23 (Belgian network on Stochastic modeling, analysis, design and optimization of communication systems, BESTCOM, 2012-2017); and Research Project FWO nr. G.091213 'Cross-layer optimization with real-time adaptive dynamic spectrum management for fourth generation broadband access networks'. P. Tsiaflakis is a postdoctoral fellow funded by the Research Foundation Flanders (FWO). The scientific responsibility is assumed by the authors.

The consequence of the time offset between the DMT blocks from different users is inter-carrier interference (ICI). With ICI, the crosstalk decoupling is broken: a tone of an interferer user affects not only the corresponding tone of a victim user, but all neighboring tones too. One fundamental step for solving the asynchronous DSM problem is an accurate characterization of the ICI. Such characterization entails calculating the ICI coefficients $\gamma_{n,i}^{k,j}\ \forall n, i, q, k,\ n \neq i$, which correspond to the crosstalk that power loaded on user i on tone j causes to user n on tone k. DSM algorithms mostly need these coefficients for the solution of the problem. Approximate characterizations lead to inaccurate power allocation, which in turn leads to suboptimal performance.

In this paper we derive a simple and accurate model for the ICI, one that takes into account all peculiarities of DMT transmission. We take into account ICI coefficients dependent on the specific delay between two users and ICI coefficients averaged over the delays between two users. We show that an accurate characterization of the ICI has a positive impact on the final performance of the system.

2. PROBLEM STATEMENT AND PREVIOUS WORK

Consider an N user DMT system with K Δ_f-spaced tones and let $\mathbf{P} = \{p_n^k\} \in \mathbb{R}^{K\times N}$ be a matrix in which p_n^k is the transmit power of user n on tone k. Let $\tilde{\sigma}_n^k$ be the background noise power observed by the user n on tone k, $h_{n,i}^k$ be the channel gain between transmitter i and receiver n at tone k and Γ be the SNR gap to capacity. The bit loading for user n on tone k in the asynchronous case is defined as

$$b_n^k = \log_2\left(1 + \frac{p_n^k}{\sigma_n^k + \mathrm{XT}_n^k}\right)$$

where

$$\mathrm{XT}_n^k = \sum_{i\neq n}^{N}\sum_{j=1}^{K} \alpha_{n,i}^{k,j} p_i^j, \tag{1}$$

$$\alpha_{n,i}^{k,j} = \frac{\Gamma\gamma_{n,i}^{k,j}|h_{n,i}^j|^2}{|h_{n,n}^k|^2} \tag{2}$$

Here $\sigma_n^k = \Gamma\tilde{\sigma}_n^k(|h_{n,n}^k|^2)^{-1}$. In (2), $\alpha_{n,i}^{k,j}$ and $\gamma_{n,i}^{k,j}$ are respectively, the normalized channel gain and the ICI coefficient specifically from user i to user n, and from tone j to tone k. In (1) XT_n^k is the total crosstalk for user n on tone k. For the synchronous case, $\gamma_{n,i}^{k,j} = 1$ for $k = j$ and zero otherwise for all users and tones. The data rate for user n is given by $R_n = f_s \sum_k b_n^k$, where f_s is the symbol rate.

The DSM problem of interest is that of finding a $\mathbf{P}$ that maximizes the weighted sum of the data rates of all users in the network given a power budget for each user, i.e.

$$\max_{\mathbf{P}} \sum_n w_n R_n, \quad \text{subject to} \quad \sum_k p_n^k \le P_n^{\max} \, \forall n \text{ and } p_n^k \ge 0 \, \forall n, k$$

Previous work on the asynchronous DSM problem includes three alternative solutions [3, 2, 4]. We will describe what seems to be the most efficient of these solutions i.e. the modified iterative waterfilling (MIW) [4], in more detail in Section 4, particularly in how this algorithm depends on the ICI coefficients.

Our goal is the accurate characterization of the ICI coefficients and an assessment of how it impacts the DSM problem. For single-user systems, the modeling of the ICI and inter-symbol interference due to an insufficient cyclic prefix (CP) length is well studied in the literature, e.g. [6]. Here, we focus on an ICI that emerges for another reason, namely the asynchronism between different users sharing the DSL network. This phenomenon was first studied in the DSL context by Chan and Yu [3] and all subsequent works followed their model. Referring to Fig. 1, consider two non-synchronized users. The delay is η, $0 \le \eta \le 1$, indicating a fraction of the DMT block length. According to [3], the ICI coefficients as a function of η are given by

$$\gamma_{n,i}^{k,j} = \begin{cases} \frac{(\eta K)^2 + (K - \eta K)^2}{K^2}, & j = k; \\ \dfrac{2 \sin^2(\pi(k-j)\eta)}{K^2 \sin^2(\pi/K(k-j))}, & j = 1, \ldots, K, \; j \ne k. \end{cases} \tag{3}$$

The authors of [3] also consider a worst case, in which the coefficients do not depend on the delay and are given by

$$\gamma_{n,i}^{k,j} = \begin{cases} 1, & j = k; \\ \dfrac{2}{K^2 \sin^2(\pi/K(k-j))}, & j = 1, \ldots, K, \; j \ne k. \end{cases} \tag{4}$$

The derivation of (3) and (4) involves a few approximations. For example, the ICI coefficients do not depend on the channel between user i and n—thus we could drop the subscripts, but we keep the same notation as in (2) for consistency—and the CP between consecutive blocks is not considered. Also note that the ICI coefficients are symmetric, i.e $\gamma_{n,i}^{(j-k),j} = \gamma_{n,i}^{j+k,j}$.

In [7, 8], the effects of ICI are studied in a wireless OFDMA scenario, where users do not overlap in frequency. According to [7], the ICI coefficients are given by

$$\gamma_{n,i}^{k,j} = \frac{1 - \cos\Big(2\pi/K(j-k)\big((K + L_{\mathrm{cp}})\nu - L_{\mathrm{cp}}\big)\Big)}{\pi^2 (j-k)^2},$$

$j = 1, \ldots, K, \; j \ne k$. Here the CP is considered—L_{cp} represents its size. Notice that, as (3) and (4), these coefficients also do not involve the channel.

In [8] the channel is considered. Because of the wireless setting, the derivation includes an expectation operation on the channel impulse response taps. These taps are considered uncorrelated and thus the model of [8] involves the power delay profile of the impulse response. The model distinguishes between five different delay situations, leading to a set of five different formulas. This approach could eventually be adapted to a situation where the channel is fixed.

3. DERIVATION OF ICI COEFFICIENTS

This section is divided in two parts. First, we obtain the ICI coefficients as a function of the delay η. Second, we obtain the ICI coefficients averaged over η.

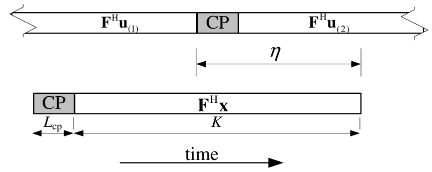

Fig. 1. DMT reception in time for victim user n.

In the following, lower-case boldface letters denote vectors, while upper-case boldface is used for matrices. When we refer to DMT symbols, bracketed subscripts refer to time (not to user) and superscripts to tones. Hence $a_{(i)}^k$ should be read as a quantity in the ith block at the kth tone. The vector $\mathbf{a}_{(i)} = \begin{bmatrix} a_{(i)}^1 & \cdots & a_{(i)}^K \end{bmatrix}^{\mathrm{T}}$ is representative for the ith symbol. The DMT block has length $K + L_{\mathrm{cp}}$, where L_{cp} is the length of the CP—we refer to a block as the symbol plus the CP. Other notation includes $\mathcal{E}[\cdot]$ as expectation, $(\cdot)^H$ as conjugate transpose, $\lfloor \cdot \rfloor$ as rounding down and $\mathrm{diag}\{\mathbf{a}\}$ as a matrix with $\mathbf{a}$ on the main diagonal. Also $\mathbf{0}_{N \times K}$ is the $N \times K$ matrix of zeros and $\mathbf{I}_K$ is the $K \times K$ identity matrix.

3.1. ICI coefficients as a function of the delay η

Referring to Fig. 1, we consider a victim user n and one interferer i. The victim user transmits a DMT symbol denoted by $\mathbf{x} \in \mathbb{C}^K$, while the interferer transmits the symbol $\mathbf{u} \in \mathbb{C}^K$. Users are not synchronized, and the delay is η, $0 \le \eta \le 1$, indicating a fraction of the DMT block length. We define η as the delay between the beginning of the CP of the interferer to the end of the DMT block of the victim user (see Fig. 1). DMT symbols $\mathbf{u}_{(1)}$ and $\mathbf{u}_{(2)}$ interfere with the reception of the victim user. Mathematically, reception for the victim user is given by

$$\begin{aligned} \mathbf{r} &= \mathbf{F}\widetilde{\mathbf{C}}\mathbf{G}_{n,n}\mathbf{C}\mathbf{F}^H\mathbf{x} + \sum_{j=1,2} \mathbf{F}\widetilde{\mathbf{C}}\mathbf{G}_{n,i}\mathbf{S}_{(j)}\mathbf{C}\mathbf{F}^H\mathbf{u}_{(j)} + \mathbf{z} \\ &= \mathrm{diag}\{\mathbf{h}_{n,n}\}\mathbf{x} + \sum_{j=1,2} \mathbf{F}\widetilde{\mathbf{C}}\mathbf{G}_{n,i}\mathbf{S}_{(j)}\mathbf{C}\mathbf{F}^H\mathbf{u}_{(j)} + \mathbf{z}. \end{aligned} \tag{5}$$

Here $\mathbf{F}$ and $\mathbf{F}^H \in \mathbb{C}^{K \times K}$ represent the DFT and IDFT matrices, respectively; $\mathbf{G}_{n,i} \in \mathbb{C}^{(K+L_{\mathrm{cp}}) \times (K+L_{\mathrm{cp}})}$ is a Toeplitz matrix with first column $\begin{bmatrix} \mathbf{g}_{n,i}^{\mathrm{T}} & \mathbf{0}_{1 \times (K+L_{\mathrm{cp}}-L)} \end{bmatrix}^{\mathrm{T}}$ and first row $\begin{bmatrix} g_{n,i}(1) & \mathbf{0}_{1 \times (K+L_{\mathrm{cp}}-1)} \end{bmatrix}$, where $\mathbf{g}_{n,i} \in \mathbb{C}^L$ is the L-tap channel impulse response from transmitter i to receiver n and is considered constant in time; $\mathbf{h}_{n,i} = \begin{bmatrix} h_{n,i}^1 & \cdots & h_{n,i}^K \end{bmatrix}^{\mathrm{T}} \in \mathbb{C}^K$ is the corresponding channel frequency response; $\mathbf{z} \in \mathbb{C}^K$ is the background Gaussian noise vector; and the matrices

$$\widetilde{\mathbf{C}} = \begin{bmatrix} \mathbf{0}_{K \times L_{\mathrm{cp}}} & \vdots & \mathbf{I}_K \end{bmatrix} \quad \text{and} \quad \mathbf{C} = \begin{bmatrix} \mathbf{0}_{L_{\mathrm{cp}} \times (K - L_{\mathrm{cp}})} & \mathbf{I}_{L_{\mathrm{cp}}} \\ \hline \multicolumn{2}{c}{\mathbf{I}_K} \end{bmatrix},$$

where $\widetilde{\mathbf{C}} \in \mathbb{R}^{K \times (K+L_{\mathrm{cp}})}$ and $\mathbf{C} \in \mathbb{R}^{(K+L_{\mathrm{cp}}) \times K}$, respectively remove and insert the CP. If $L_{\mathrm{cp}} \ge L$, the operation $\widetilde{\mathbf{C}}\mathbf{G}_{n,n}\mathbf{C}$ results in a square circulant matrix, which is then diagonalized by pre- and post-multiplication with the IDFT and DFT matrices. We assume that the CP is longer than both the direct and crosstalk channel impulse response.

The matrices $\mathbf{S}_{(1)}$ and $\mathbf{S}_{(2)}$ capture the effect of the time offset. Define $\omega = \lfloor \eta(K + L_{\mathrm{cp}}) \rfloor$ as the number of samples in delay. These matrices are given by

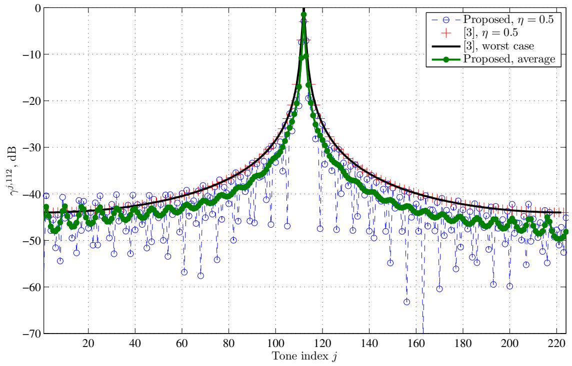

Fig. 2. ICI coefficients from (11), (3) and (4). For the first two plots, $\eta = 0.5$. The crosstalk channel is 1 km long.

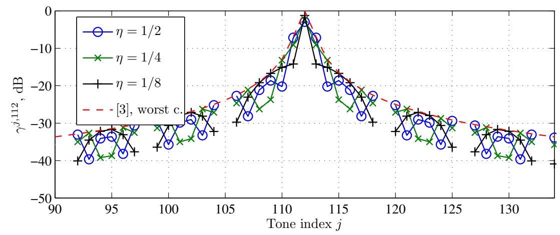

Fig. 3. ICI coefficients for different values of the delay η. In this plot we consider a frequency flat channel.

$$\mathbf{S}_{(1)} = \left[\begin{array}{c|c} \mathbf{0}_{(K+L_{\rm cp}-\omega)\times\omega} & \mathbf{I}_{(K+L_{\rm cp}-\omega)} \\ \hline \multicolumn{2}{c}{\mathbf{0}_{\omega\times(K+L_{\rm cp})}} \end{array}\right] \tag{6}$$

and

$$\mathbf{S}_{(2)} = \left[\begin{array}{c|c} \multicolumn{2}{c}{\mathbf{0}_{(K+L_{\rm cp}-\omega)\times(K+L_{\rm cp})}} \\ \hline \mathbf{I}_{\omega} & \mathbf{0}_{\omega\times(K+L_{\rm cp}-\omega)} \end{array}\right]. \tag{7}$$

Here $\mathbf{S}_{(1)},\ \mathbf{S}_{(2)} \in \mathbb{N}^{(K+L_{\rm cp})\times(K+L_{\rm cp})}$. If η is equal to zero or one, then the system is synchronized and $\mathbf{S}_{(1)} = \mathbf{I}_{(K+L_{\rm cp})}$ and $\mathbf{S}_{(2)} = \mathbf{0}_{(K+L_{\rm cp})\times(K+L_{\rm cp})}$ or vice-versa. For $0 < \eta < 1$, the operation $\widetilde{\mathbf{C}}\mathbf{G}_{n,i}\mathbf{S}_{(1)}\mathbf{C}$ (and $\widetilde{\mathbf{C}}\mathbf{G}_{n,i}\mathbf{S}_{(2)}\mathbf{C}$) fails to produce a circulant matrix, and therein lies the effect of the asynchronicity.

Observe that we can write one element of $\mathbf{r}$ in (5) as

$$r^k = h^k_{n,n}x^k + \sum_j \mathbf{A}_{n,i}[k,j]u^j_{(1)} + \sum_j \mathbf{B}_{n,i}[k,j]u^j_{(2)} + z^k.$$

Here the $[k,j]$ elements of $\mathbf{A}_{n,i}$ and $\mathbf{B}_{n,i}$ account for the ICI effect when $j \neq k$. These matrices are defined as

$$\mathbf{A}_{n,i} = \mathbf{F}\widetilde{\mathbf{C}}\mathbf{G}_{n,i}\mathbf{S}_{(1)}\mathbf{C}\mathbf{F}^H, \tag{8}$$

$$\mathbf{B}_{n,i} = \mathbf{F}\widetilde{\mathbf{C}}\mathbf{G}_{n,i}\mathbf{S}_{(2)}\mathbf{C}\mathbf{F}^H. \tag{9}$$

With (8) and (9) in hands and taking into account that the PSD of the crosstalk symbols is $\mathrm{E}\big[\mathbf{u}_{(1)}\mathbf{u}^H_{(1)}\big] = \mathrm{E}\big[\mathbf{u}_{(2)}\mathbf{u}^H_{(2)}\big] = \mathrm{diag}\{\mathbf{p}_i\}$, we can write

$$\gamma^{k,j}_{n,i}|h^j_{n,i}|^2 p^j_i = \left(|\mathbf{A}_{n,i}[k,j]|^2 + |\mathbf{B}_{n,i}[k,j]|^2\right) p^j_i. \tag{10}$$

Eq. (10) is easily calculable and it offers an accurate model for the ICI as a function of $\mathbf{g}_{n,i}$ and η. Note that (10) accounts for all possible delay situations. This is in contrast with [8], where the derivation of the ICI coefficients is sub-divided in five different situations depending on the delay, which results in five different formulas. Furthermore, the derivation of (10) is simpler and does not need the addition of unnecessary variables—for example, in [8], a variable is introduced to account for how many channel taps should be included in the calculation.

For comparing the ICI coefficients to those of [3], we want the ICI PSD to be captured by a multiplication of the type $\mathbf{M}_{n,i}\times \mathrm{diag}\big\{|\mathbf{h}_{n,i}|^2\big\}\mathrm{diag}\{\mathbf{p}_i\}$, where $\mathbf{M}_{n,i} \in \mathbb{R}^{K\times K}$ is the ICI coefficients matrix and $|\mathbf{h}_{n,i}|^2 = \big[|h^1_{n,i}|^2 \ \cdots \ |h^K_{n,i}|^2\big]^{\rm T} \in \mathbb{R}^K$. If we follow the notation of [3], each row of $\mathbf{M}_{n,i}$ would contain the ICI coefficients for one victim tone, i.e. $\mathbf{M}_{n,i} = \big[\boldsymbol{\gamma}^1_{n,i}\ \boldsymbol{\gamma}^2_{n,i} \ \cdots \ \boldsymbol{\gamma}^K_{n,i}\big]$, where $\boldsymbol{\gamma}^k_{n,i} = \big[\gamma^{1,k}_{n,i} \ \cdots \ \gamma^{K,k}_{n,i}\big]^{\rm T}$. Calculating the PSD of the interference term in (5), we obtain

$$\mathbf{M}_{n,i}\mathrm{diag}\big\{|\mathbf{h}_{n,i}|^2\big\}\mathrm{diag}\{\mathbf{p}_i\} =$$
$$\left(|\mathbf{F}\widetilde{\mathbf{C}}\mathbf{G}_{n,i}\mathbf{S}_{(1)}\mathbf{C}\mathbf{F}^H|^2 + |\mathbf{F}\widetilde{\mathbf{C}}\mathbf{G}_{n,i}\mathbf{S}_{(2)}\mathbf{C}\mathbf{F}^H|^2\right)\mathrm{diag}\{\mathbf{p}_i\},$$

and hence

$$\mathbf{M}_{n,i} = \left(|\mathbf{A}_{n,i}|^2 + |\mathbf{B}_{n,i}|^2\right)\mathrm{diag}\big\{|\mathbf{h}_{n,i}|^2\big\}^{-1}, \tag{11}$$

where $\mathbf{A}_{n,i}$ and $\mathbf{B}_{n,i}$ are defined in (8) and (9) and where the $[k,j]$th element of $|\mathbf{A}_{n,i}|$ is $|\mathbf{A}_{n,i}[k,j]|$.

With $\mathbf{M}_{n,i}$ calculated as in (11) we can calculate $\alpha^{k,j}_{n,i}$ with (2) and crosstalk (1). Notice that we need the crosstalk channel impulse response, $\mathbf{g}_{n,i}$, to compute (10) or (11). As a consequence, the ICI coefficients are channel dependent, i.e. different crosstalk channels have different ICI coefficients. They are also frequency dependent: the columns of $\mathbf{M}_{n,i}$ are similar, but they are not delayed replicas of one another, e.g. $\gamma^{k,j}_{n,i}$ is usually slightly different than $\gamma^{k+1,j+1}_{n,i}$. It can be shown that the only exception to these two facts is the case of frequency flat channels, i.e. when $\mathbf{g}_{n,i} = \big[\nu \ \mathbf{0}_{K+L_{\rm cp}-1\times 1}\big]^{\rm T}$ for a given complex number ν. Notice that in this case $\mathbf{G}_{n,i} = \nu\mathbf{I}_K$. For the frequency flat case, the ICI coefficients are also not frequency dependent, i.e. $\gamma^{k,j}_{n,i} = \gamma^{k+1,j+1}_{n,i}$.

In Fig. 2, we plot the ICI coefficients for tone 112 of the 224 tones of an ADSL downstream system with AWG 24 cable for a delay of $\eta = 0.5$. The crosstalk channel for this example is 1 km long and was calculated according to [9]. We use a CP of 32 samples [10]. The plot shows ICI coefficients calculated with (3) and (4), following the model of [3]; and (11) in this paper. Observe that the coefficients of (3) for $\eta = 0.5$ are usually optimistic and the coefficients of (4) for the worst case are usually pessimistic.

In Fig. 3, we illustrate the change in the coefficients when we vary η for tone 112 of the 224 tones for the same ADSL system. For this plot, we assume a frequency flat crosstalk channel. We also only show the ICI coefficients of the 12 closest tones. As mentioned, the coefficients are now symmetric and not frequency dependent. In this same figure, we again show the worst case model of (4). In this frequency flat situation, the formula of [7] would give the same results as ours.

3.2. ICI coefficients averaged over η

In the previous section η was considered a fixed variable. In this section, we consider it to be a random variable, and we calculate the crosstalk as the expected value of a function of η. Let $\mathbf{M}_{n,i}(\eta)$ be a function of the random variable η. It is defined similarly to (11), i.e.

$$\mathbf{M}_{n,i}(\eta) = \left(|\mathbf{A}_{n,i}|^2 + |\mathbf{B}_{n,i}|^2\right)\mathrm{diag}\{|\mathbf{h}_{n,i}|^2\}^{-1}.$$

We remind that the dependence on the delay η is through the definition of (6) and (7). Also, let $f_\eta(H)$ be a given probability distribution function. The expected value of $\mathbf{M}_{n,i}(\eta)$ is given by [11]

$$\mathcal{E}\left[\mathbf{M}_{n,i}(\eta)\right] = \int_{-\infty}^{+\infty} \mathbf{M}_{n,i}(H) f_\eta(H) dH. \tag{12}$$

We can rewrite (12) in a more convenient form by noticing that the matrices $\mathbf{S}_{(1)}$ and $\mathbf{S}_{(2)}$ in (6) and (7) depend on $\lfloor \eta(K + L_{\text{cp}}) \rfloor$. Hence, we define a discrete random variable $\omega = \lfloor \eta(K+L_{\text{cp}}) \rfloor$. We consider that η is uniformly distributed between 0 and 1, which leads us to conclude that ω is also uniformly distributed. Mathematically, we have $\Pr(\omega = \Omega) = {}^{1}/_{K+L_{\text{cp}}},\ \Omega = \{0, 1, \ldots, K + L_{\text{cp}} - 1\}$. In this way, we can rewrite (12) as a simple average, i.e.

$$\widetilde{\mathbf{M}}_{n,i} \triangleq \mathcal{E}\left[\mathbf{M}_{n,i}(\omega)\right] = \sum_{\Omega=0}^{K+L_{\text{cp}}-1} \mathbf{M}_{n,i}(\Omega) \frac{1}{K + L_{\text{cp}}}. \tag{13}$$

With $\widetilde{\mathbf{M}}_{n,i}$ in hands, we can calculate crosstalk with (2) and (1). In Fig. 2, we plot the ICI coefficients of (13) for tone 112 of the same 1 km crosstalk channel mentioned on Section 3.1.

Eq. (13) is useful because it is independent of the specific delay between two users. Calculating the ICI coefficients with (13) may be more interesting, since it is likely that the delay between the transmission of two users changes over time and is not known accurately.

4. EXPERIMENTS

In this section, we illustrate how an accurate characterization of the ICI coefficients impacts on performance. For assessing this impact, we use the MIW algorithm [4]. Power allocation for the MIW is done with the formula

$$p_i^j = \frac{w_i}{\lambda_i + t_i^j} - (\sigma_i^j + \mathrm{XT}_i^j), \tag{14}$$

where

$$t_i^j = \sum_{n \neq i} w_n \sum_k \frac{\alpha_{n,i}^{k,j} (\mathrm{SINR}_n^k)^2}{p_n^k (\mathrm{SINR}_n^k + 1)} \tag{15}$$

Here $\mathrm{SINR}_n^k = p_n^k \left(\sigma_n^k + \mathrm{XT}_n^k\right)^{-1}$. In (14), λ_n is a Lagrange multiplier that is adjusted so that the power budget is respected. The variable t_i^j is a per-tone penalty that considers damage to other users.

The MIW can be applied in a distributed fashion in the network. Users can apply (14) locally. After power allocation, users measure their SINR's, calculate $(\mathrm{SINR}_n^k)^2 \left(p_n^k (\mathrm{SINR}_n^k + 1)\right)^{-1}$ for every tone and send these values to a spectrum management center (SMC). The SMC then calculates the per-tone penalties with (15) for all users and tones and sends these values to the users. The process repeats until convergence. Note that users can measure their SNIR's accurately without the knowledge of the ICI coefficients, but the SMC needs accurate values for the ICI coefficients $\gamma_{n,i}^{k,j}$, which in turn define $\alpha_{n,i}^{k,j}$ (see (15) and (2)). Inaccurate ICI coefficients on the SMC can lead to inaccurate values for the per-tone penalties, which in turn influences the power allocation and performance.

In this section, we assess the performance of the MIW for three cases. First, we consider the case when the delay η is known for every user pair, the accurate ICI coefficients are calculated with (11) and used at the SMC; second, we consider the case when the delay is not known, the averaged ICI coefficients are calculated with (13) and used at the SMC; and, third, we consider the case when the delay is not known, the worst case ICI coefficients in (4) are calculated and used at the SMC. All simulations in this section consider a standard downstream ADSL scenario.

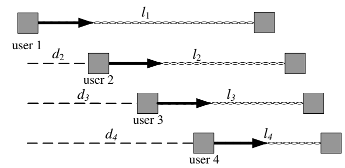

Fig. 4. Near-far downstream ADSL scenario.

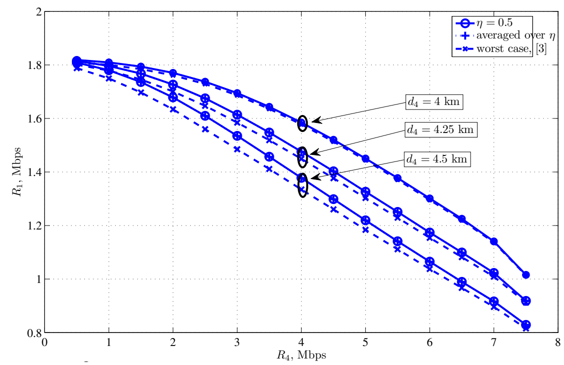

Fig. 5. Rate region for the scenario of interest.

The scenario consists of 4 users. See Fig. 4. Define the vectors $\mathbf{l} = \left[l_1\ \cdots\ l_4\right]^{\mathrm{T}} = \left[5\ 4\ 3.5\ 3\right]^{\mathrm{T}}$ km, and $\mathbf{d} = \left[d_1\ \cdots\ d_4\right]^{\mathrm{T}} = \left[0\ 2\ 3\ d_4\right]^{\mathrm{T}}$. We simulate three different values for d_4, $d_4 = 4$, $d_4 = 4.25$ and $d_4 = 4.5$ km.

Consider the delay between user i and n to be given by $\eta_{n,i}$. We consider users 1 and 2 to be synchronized, so $\eta_{1,2} = \eta_{2,1} = 0$. We also consider $\eta_{3,4} = \eta_{4,3} = 0$. Users 1 and 2 have a delay of 0.5 in relation to users 3 and 4, so $\eta_{4,1} = \eta_{1,4} = 0.5$, $\eta_{3,2} = \eta_{2,3} = 0.5$ and so on.

We depict the rate regions for the three cases of interest regarding the knowledge of the ICI coefficients on the SMC and for the three different values of d_4 in Fig. 5 . For all points, we have $R_2 = 2$ Mbps and $R_3 = 3$ Mbps. As we can see from the plot, using the averaged ICI coefficients on the SMC provides a performance which is practically the same as that using the actual coefficients. This suggests that the accurate (non-averaged) coefficients may not be all the time strictly necessary. Performance is clearly worse with the worst case ICI coefficients. For $d_4 = 4.5$ km, the difference can be up to 10 %.

5. CONCLUSION

Previous work on DSM has mostly focused on the synchronous transmission case, which makes the problem easier but not always realistic. In this paper, we have focused on the asynchronous DSM problem. We have provided a simple and accurate ICI characterization for the asynchronous DMT transmission in DSL networks, as well as an ICI characterization averaged over the possible delays between two users. Simulation results show that an accurate characterization of the ICI coefficients can has a positive impact on the performance of distributed DSM algorithms.

6. REFERENCES

[1] F. Sjöberg, M. Isaksson, R. Nilsson, P. Ödling, S. K. Wilson, and P. O. Börjesson, "Zipper: A duplex method for VDSL based on DMT," *IEEE Trans. Commun.*, vol. 47, no. 8, pp. 1245–1252, 1999.

[2] R. Cendrillon, J. Huang, M. Chiang, and M. Moonen, "Autonomous spectrum balancing for digital subscriber lines," *IEEE Trans. Signal Process.*, vol. 55, no. 8, pp. 4241–4257, 2007.

[3] V. M. K. Chan and W. Yu, "Multiuser spectrum optimization for discrete multitone systems with asynchronous crosstalk," *IEEE Trans. Signal Process.*, vol. 55, no. 11, pp. 5425–5435, 2007.

[4] W. Yu, "Multiuser water-filling in the presence of crosstalk," in *Inf. Theory and Appl. Workshop*, San Diego, USA, 2007.

[5] R. B. Moraes, P. Tsiaflakis, and M. Moonen, "Dynamic spectrum management in DSL with asynchrnous crosstalk," in *IEEE Int. Conf. Acoust., Speech, Signal Process.*, Prague, Czech Republic, 2011.

[6] W. Henkel, G. Tauböck, P. Ödling, P. O. Börjesson, and N. Petersson, "The cyclic prefix of OFDM/DMT—an analysis," in *Int. Zurich Seminar on Broadband Commun.*, Zurich, Switzerland, 2002.

[7] M. Park, K. Ko, H. Yoo, and D. Hong, "Performance analysis of OFDMA uplink systems with symbol timing misalignment," *IEEE Trans. Commun.*, vol. 7, no. 8, pp. 376–378, 2003.

[8] M. Park, K. Ko, B. Park, and D. Hong, "Effects of asynchronous MAI on average SEP performance of OFDMA uplink systems over frequency-selective rayleigh fading channels," *IEEE Trans. Commun.*, vol. 58, no. 2, pp. 586–599, 2010.

[9] ETSI Std. TS 101 270-1, "Transmission and multiplexing (TM); acess transmission systems on matellic acess cables; very-high bit-rate digital subscriber line transceivers (VDSL); part 1: Functional requirements," 2003.

[10] ITU std. G.992.2, "Asymmetrical digital subscriber line transceivers 2 (ADSL2)," 2002.

[11] A. Papoulis and S. U. Pillai, *Probability, Random Variables and Stochastic Processes*, 4th ed. McGraw-Hill Inc., New York, 2001.